

Wool keratin film plasticized by citric acid for food packaging

*Diego O. Sanchez Ramirez**, *Riccardo A. Carletto*, *Cinzia Tonetti*, *Francesca Truffa Giachet*,

*Alessio Varesano**, *Claudia Vineis*

Institute for Macromolecular Studies, National Research Council of Italy (CNR-ISMAL), Corso
Giuseppe Pella 16, I-13900 Biella, Italy.

*Corresponding Author:

Tel. (+39) 015 849 30 43

Fax (+39) 015 840 83 87

Diego O. Sanchez Ramirez (E-mail: do.sanchezramirez@bi.ismac.cnr.it).

Alessio Varesano (E-mail: a.varesano@bi.ismac.cnr.it)

1 **ABSTRACT**

2 Wool keratin (natural resource) and citric acid (effective preservative) were mixed in water to
3 produce a transparent film for application in active packaging. This film showed excellent biocidal
4 effect, high elongation value (600 %) and little loss of keratin after immersion in water. [The](#)
5 [capability of citric acid to bind keratin macromolecules by hydrogen bonds is probably responsible](#)
6 [for the improvement of film's extensibility](#). On the other hand, the study of FT-IR spectrum allows
7 understanding that the presence of citric acid in aqueous solution enhances the content of alpha
8 helix structure in the film, with a reduction in the amount of side chain and disordered
9 conformations in the macromolecular structure. Carrot shelf-life was qualitatively improved with
10 this film in comparison with a commercial film for preserving food. Consequently, this film can
11 have possible application for food packaging as a substitute of synthetic polymers replacing them
12 with a natural, environmental friendly and renewable resource.

13 **KEYWORDS:** packaging, keratin, citric acid, protein, plasticizer.

14 1. Introduction

15 Innovative packaging materials that can extend the shelf-life, maintaining consumer safety,
16 reducing losses to the production sector and being environmental friendly, has been the focus of
17 extensive efforts. Particularly, biopolymers such as lipids, proteins, polysaccharides and mixtures
18 thereof, have been investigated to enhance the properties of films as packaging materials (Caro,
19 Medina, Díaz-Dosque, López & Abugoch, 2016). There is a current trend to incorporate active
20 agents into packaging materials, to maintain the quality and to enhance the safety of packaged
21 foods (Fabra, López-Rubio & Lagaron, 2016). In food technology, active packaging with
22 antibacterial property is a concept based on incorporating an antimicrobial compound inside the
23 packaging material or using a packaging material with inherent antimicrobial properties to reduce
24 or inhibit microbial growth (Appendini & Hotchkiss, 2002).

25 Traditionally, antimicrobial agents are directly mixed into the initial food formulations, but this
26 direct addition may change the taste of the food and result in the inactivation or evaporation of
27 active agents with rapid migration into the bulk of the foods; consequently, antimicrobial activity
28 is rapidly lost. As antimicrobial packaging materials must contact the surface of food, the
29 antimicrobial agents could spread out to its surface, enhancing the shelf-life and safety of packaged
30 food (Long, Joly & Dantigny, 2016).

31 Keratin is a natural protein extracted from wool or other natural resource (Fraser, MacRae, &
32 Rogers, 1972). In different works it has been used to produce nanofibers (Varesano et al., 2015;

33 Varesano, Vineis, Tonetti, Sanchez Ramirez & Mazzuchetti, 2014; Aluigi, Corbellini,
34 Rombaldoni, Zoccola & Canetti, 2013) because of its special absorption properties of metal ions
35 like Cu (Aluigi, Tonetti, Vineis, Tonin, & Mazzuchetti, 2011), Cr (Aluigi et al., 2012; Aluigi,
36 Vineis, Tonin, Tonetti, Varesano & Mazzuchetti, 2009), dyes like methylene blue (Aluigi,

37 Rombaldoni, Tonetti & Jannoke, 2014) and volatile organic compounds like formaldehyde
38 (Aluigi, Vineis, Tonin, Tonetti, Varesano & Mazzuchetti, 2009) and because of its possible
39 applications as scaffolds for human body (Tachibana, Furuta, Takeshima, Tanabe & Yamauchi,
40 2002; Tachibana, Kaneko, Tanabe & Yamauchi, 2005) thanks to its biodegradability (Yamauchi,
41 Maniwa & Mori, 1998). Unfortunately, keratin has not good mechanical properties, so it is
42 necessary to use it in blend with a synthetic and not biodegradable polymer (Aluigi, Tonetti,
43 Vineis, Tonin, & Mazzuchetti, 2011; Aluigi, Vineis, Tonin, Tonetti, Varesano & Mazzuchetti,
44 2009).

45 On the other hand, it is possible to find several works where citric acid was employed with
46 natural polymers as compatibilizer and plasticizer to improve the mechanical properties of films.
47 In fact, citric acid has properties to form stronger hydrogen bonds with hydroxyl groups to prevent
48 recrystallization and to enhance the interactions between molecules in polymers as [polyvinyl](#)
49 [alcohol, starch and polycaprolactone](#) (Ortega-Toro, Collazo-Bigliardi, Talens & Chiralt, 2016;
50 Ghanbarzadeh, Almasi & Entezami, 2011; Reddy & Yang, 2010; Shi et al., 2008; Jiugao, Ning &
51 Xiafoei, 2005). In addition, citric acid has antibacterial properties (In, Kim, Kim & Oh, 2013;
52 Pundir, & Jain, 2011) and it is used in many different products to preserve different types of food
53 (Pundir, & Jain, 2011; Soccol, Vandenberghe, Rodrigues & Pandey, 2006). The aim of this work
54 is to obtain a film produced by casting using citric acid and keratin in aqueous solution, to use it
55 in food industry as an active packaging because of its antimicrobial activity and plasticizer
56 property. The film was analyzed by means of TGA, DSC and FT-IR. Moreover, strength tension,
57 elongation at break, antibacterial efficiency, transparency and loss of weight after immersion in
58 water were measured. Finally, the carrot shelf-life preserved with the keratin-citric acid film was
59 qualitatively evaluated and compared with one of the commercial films for food packaging.

60

61 **2. Materials and Methods**

62 *2.1. Keratin extraction and purification*

63 Keratin was extracted from wool by sulfitolysis with sodium metabisulfite (Aluigi et al., 2007).
64 Preliminarily, the wool fibers were cleaned by Soxhlet extraction with petroleum ether to remove
65 fatty matter and washed with distilled water. An amount of 15 g of cleaned fibers were cut into
66 snippets and treated with 300 ml of a solution containing urea (8M) and sodium metabisulfite
67 (0.5M), adjusted to pH 6.5 with sodium hydroxide (5N), under shaking for 2 h at 65 °C. The
68 mixture was filtered with 30 µm and then 5 µm pore-size filters, and the keratin aqueous solution
69 obtained was dialyzed against distilled water with a cellulose tube (3.500-Da molecular weight
70 cutoff) for 3 days at room temperature, changing the distilled water frequently. The keratin solution
71 was frozen and then lyophilized with a Heto PowerDry PL3000 freeze dryer to obtain soluble and
72 pure keratin.

73 Citric acid (99 %) was purchased from Sigma Aldrich. Citric acid and keratin were dissolved in
74 distilled water to obtain a final concentration of 15 % wt. of keratin and 10% wt. of citric acid. The
75 solution was shaken until dissolution by means of a magnetic stirrer ensuring its completed
76 homogeneity. After that, 3 ml of solution was poured in a polyethylene bowl and dried at 20 °C
77 and 65 %RH to form a film by casting. The film was separated from the support and cut in a
78 rectangular form of 1 x 2 cm. The same volume of solution and bowl dimension was maintained
79 for each test to standardize the production process.

80 *2.2. UV-VIS (transparency and immersion in water)*

81 In order to measure the keratin-citric acid film transparency, an analysis employing UV-Visible
82 Spectrometer (Lamba 35 PerkinElmer) between 200 and 700 nm was carried out. In addition,
83 sample pictures of film were taken with a camera.

84 Samples (0.1 g) were immersed in 5 and 20 ml of water up to 170 h in order to verify the water
85 stability. The water after film immersion was qualitative analyzed in UV-Visible spectrometer
86 between 200 and 700 nm. The intensity of peaks were measured at different immersion times. In
87 addition, gravimetric analyses at different times (between 5 min to 2 h) were carried out measuring
88 the loss of weight in the dried samples; the quantification of protein in solution was realized with
89 Bio-Rad Protein Assay (Micro Assay) based on the Bradford method. The Protein Assay Dye
90 Reagent Concentrate with one standard (Bovine Serum Albumin) were purchased from Bio Rad.

91 The dry weight was measured using the moisture analyzer DBS 60-3 equipped with a Halogen
92 quartz glass heater 400W. The measurements were carried out in Drying mode AUTO (standard
93 drying), where the drying temperature was set at 105°C and the drying process was finished
94 automatically when the present weight loss remained constant for 30 seconds.

95 In addition, the pH of water after film immersion was measured with a PC 8 Instrumental Bench
96 (pH/mV/COND/TDS/°C) – CARLI Biotec equipped with a polymer electrode type (Basic Pro
97 pH).

98 *2.3. Thermal treatments*

99 Some samples were heated in an oven to study the effect of annealing on the mechanical
100 properties of film. These were subjected to heat treatments in air at different temperatures (80, 100
101 and 120°C) for one hour. Samples were conditioned for at least 24 h at 20 °C and 65% RH before
102 and after each heat treatment.

103 *2.4. TGA and DSC analysis*

104 The thermogravimetric analysis was done with a Mettler Toledo TGA-DSC. About 2.5 mg of
105 film was put in a 70 ml aluminum oxide crucible for the analysis. The calorimeter cell was flushed
106 with nitrogen at 70 ml min⁻¹. The TGA data were elaborated with a Mettler Toledo STARe system.
107 The run was performed from 30 to 500 °C with a heating rate of 10 °C min⁻¹. Derivative
108 thermogravimetry (DTG) was used to identify the temperature of maximum mass-loss rates.

109 Differential scanning calorimetry (DSC) was performed with a Mettler Toledo DSC calorimeter
110 calibrated by an indium standard. The calorimeter cell was flushed with 100 ml min⁻¹ nitrogen.
111 The run was performed from 30 to 450 °C, at the heating rate of 10 °C min⁻¹. The mass was close
112 to 2.5 mg of sample.

113 *2.5. Mechanical tests and thickness measurement*

114 In order to evaluate tensile strength and elongation at break an Instron (USA) 5500R tensile
115 testing machine, configured with a 10 N load cell with a velocity of 10 mm min⁻¹ was used.

116 Scanning electron microscopy (SEM) instrument was used to make a measurement of thickness
117 in seven different samples on eight different points for each of them. Measurements were carried
118 out with a LEO (Leica Electron Optics) 435 VP SEM. Operative parameters were 15 kV
119 acceleration voltage and 30 mm working distance. Specimens were sputter-coated with gold before
120 SEM analysis in an Emitech K550 Sputter Coater with a current of 20 mA for 5 minutes in rarefied
121 argon at 20 Pa.

122 *2.6. FT-IR analysis*

123 IR spectra were recorded with a Thermo Nicolet Nexus spectrometer by an attenuated total
124 reflection technique with a Smart Endurance accessory (equipped with a diamond crystal ZnSe
125 focusing element) in the range from 4000 to 550 cm⁻¹ with 50 scans and 4 cm⁻¹ band resolution.
126 Ommic 6.2 software (by Thermo Electron) was used to perform attenuated total reflection baseline

127 correction. Tests were performed on several parts of each sample to evaluate the citric acid
128 distribution homogeneity.

129 2.7. Antibacterial test

130 Antibacterial tests were performed employing the gram positive *Staphylococcus aureus* by using
131 AATCC 100 Test Method. In the procedure was used 1 ml of bacteria standardized inoculum
132 containing $1.5-3 \times 10^5$ CFU ml⁻¹ on the sample. After one hour 100 ml of sterile buffer were added
133 on the sample, the buffer was then diluted ten times and plated on Petri dishes with suitable agar.
134 The Petri dish was incubated at least 24 h at 37 °C, then the bacteria colonies were counted.
135 Bacterial reduction is calculated as $((B - A) / B) * 100$, where A is the number of colonies of the
136 sample with the film and B is the number of colonies of the sample without film (reference).

137 2.8. Qualitative assessment of carrot shelf-life

138 Carrots pieces were stored on the laboratory bench at 20 °C of temperature and 65% of humidity.
139 In order to realize the quality assessment of carrot shelf-life, the different pieces of carrot were
140 packed in a film for preserving food and keratin/citric acid film; then they were compared with a
141 piece unpacked in any film. The film for preserving food was a commercial PET film. Carrot was
142 acquired from a local orchard and was chosen as a sample of food to test the film because its
143 availability and organic origin.

144

145 3. Results and Discussions

146 3.1. UV-VIS (transparency and water immersion)

147 Figure 1(a) shows the spectrum UV-VIS of the keratin/citric acid film. In the visible range (400
148 – 700 nm) the film has low absorbance value (close to 0.4), whilst in UV range the film has two
149 strong peaks. The first one at 220 nm related by the carboxylic acid and/or amino groups of peptide

150 bonds and the second one at 280 nm caused by the aromatic ring portion of amino acids groups
151 (Schmid, 2001; Hegyi et al., 2013; Held, 2016). Figure 1(b) reports a picture of the keratin/citric
152 acid film that shows good property of transparency.

153 Figure 2 shows the absorbance values of water after the immersion of keratin/citric acid film at
154 275 nm (Figure 2 (a)) and 214 nm (Figure 2 (b)). On the one hand, in the Figure 2 (a), the signal
155 of aromatic ring of amino acids groups from peptides chains is reported. This figure qualitatively
156 confirms the presence of protein chains in water and shows that the amount of peptide chain
157 increases considerably after 50 h reaching the maximum value at 100 h. At 170 h the absorbance
158 value probably decreased as consequence of the degradation of phenylalanine and tyrosine amino
159 acids groups in the keratin chain. On the other hand, in the Figure 2 (b), the signal of carboxylic
160 acid and/or amino groups of peptide bonds is reported. Unlike in the previous one, the peak can be
161 the result of the contribution of carboxylic groups present in the citric acid and peptide bonds. As
162 a result, the second figure shows a constant trend in time, mainly caused by the citric acid release
163 of film that could hide the signal of peptide bonds.

164 Table 1 reports the average results of keratin/citric acid film water immersion measured at 5, 10,
165 15, 30, 1 h and 2 h. After 5 min the parameters of the solutions reached approximatively a constant
166 value with slight changes until 2 h.

167 As shown in Table 1, the amount of lost keratin decreased and the mean value of lost citric acid
168 increased when the volume was reduced from 20 to 5 ml, but the total loss of weight remained
169 constant at ~55 % wt.. Moreover, considering both the sample volumes, the citric acid contained
170 in the film was almost completely released while the keratin released was 12 % wt. in 20 ml and
171 6 % wt. in 5 ml. Therefore, the volume of water contacting the film slightly alter the process of
172 keratin release due to the saturation of the solution. It is worth noting that the protein concentration

173 reached values lower than 0.5 g l^{-1} in both the cases. The pH values slightly change with the
174 volume of water leading a more acid solution using 5 ml, as expected.

175 3.2. TGA and DSC analyses

176 In the Figure 3, it is possible to see the thermal behavior differences between pure keratin and
177 film. The pure keratin is thermally more stable than the film (Figure 3(a)): two temperatures with
178 the greatest weight loss are visible before thermal degradation starting at $248 \text{ }^\circ\text{C}$. Figure 3 shows
179 the first event with difference in the temperature of water evaporation: $60 \text{ }^\circ\text{C}$ for pure keratin
180 (Figure 3(b)) and $80 \text{ }^\circ\text{C}$ for film (Figure 3(c)). It occurs probably because of higher amount of
181 alpha helix conformations in the film that bonded water in the protein chains stronger than pure
182 keratin (Aluigi et al., 2007). The second event at $224 \text{ }^\circ\text{C}$ for pure keratin (Figure 3(b)) and $195 \text{ }^\circ\text{C}$
183 for film (Figure 3(c)), represents the maximum rate of keratin chain decomposition. In the film
184 case, it is overlapped with citric acid degradation, which starts at $155 \text{ }^\circ\text{C}$; the maximum
185 decomposition is reached at $230 \text{ }^\circ\text{C}$ and the melting point at $\sim 157 \text{ }^\circ\text{C}$ (Barbooti & Al-Sammerrai,
186 1986). In addition, the onset of this decomposition is $198 \text{ }^\circ\text{C}$ for pure keratin (Figure 3(b)) and 150
187 $^\circ\text{C}$ for film (Figure 3(c)). The differences are probably due to the citric acid decomposition
188 temperature that is close to $150 \text{ }^\circ\text{C}$. In the keratin/citric acid film, the maximum loss of weight is
189 lower ($195 \text{ }^\circ\text{C}$) than that of pure keratin ($224 \text{ }^\circ\text{C}$). As a result, the melting points change for citric
190 acid from $157 \text{ }^\circ\text{C}$ to $153 \text{ }^\circ\text{C}$ and for the keratin from $227 \text{ }^\circ\text{C}$ to $198 \text{ }^\circ\text{C}$ (Figure 3(d) and 3(e)). From
191 this point of view, it is probable that citric acid acts like a catalyzer of thermal degradation (as
192 happens in metabolism process) or produces molecules that allow degrading the keratin. In fact,
193 the heat flow is always lower for film than for pure keratin (less endothermic process).

194 Thermal analysis also shows that the beginning of thermal denaturation probably occurs between
195 $130 \text{ }^\circ\text{C}$ and $150 \text{ }^\circ\text{C}$ (Figure 3(c)); in correspondence of this temperature range, the film loses its

196 mechanical properties. In addition, there is not considerable alteration before 123 °C: before this
197 value, it is possible to avoid any denaturation in the protein chain.

198 Consequently, the temperature range between 80 and 120 °C would be an interval where occurs
199 the plasticization process of protein film. Probably, between these temperatures, the protein chain
200 starts the reticulation process which permits a variation in molecular structures contained in the
201 film; furthermore it changes the moisture contained in it. Obviously, this has consequences in the
202 enhancement of tensile strength and elongation of the film because of annealing-induced
203 phenomena.

204 *3.3. Mechanical test*

205 A mean thickness of 0.067 ± 0.034 mm was obtained from seven different samples. It was used
206 to calculate the tensile strength (Table 2). Figure 4 shows pictures during a tensile stress test of the
207 film without thermal treatment at the beginning of the test and just before its breaking.

208 In the Table 2 are reported mean values of tensile strength and elongation at break corresponding
209 with three different treatment conditions. The data show that the value of elongation at break is
210 very high. Nonetheless, this property could be reduced almost six times from the initial value by
211 using thermal treatment, with a reduction of standard deviation. The value of tension increased
212 five times from the initial value and this growth caused a decrease in the film elongation. The
213 probable cause is that thermal treatment improved tension strength: the movement of molecular
214 chain is not free anymore, due to the presence of the reticulation chain generated by the heating.
215 On the other hand, the values of elongation at break are confrontable to some commercial and
216 semi-commercial biobased materials (such as polylactate, wheat starch and corn starch) or
217 comparable to conventional materials such as LDPE and HDPE (Petersen, Nielsen & Olsen, 2001).

218 *3.4. FT-IR analyses*

219 In Figure 5 are reported the spectra of the film compared to pure keratin and pure citric acid. In
220 the spectrum of keratin, the absorption bands related to peptide bonds are shown. The amide A
221 band at 3310 cm^{-1} was assigned to the stretching vibrations of N-H bonds. The amide I band at
222 1650 cm^{-1} and the amide II at 1540 cm^{-1} were related to the stretching vibrations of C=O bonds,
223 and to the in plane bending modes of N-H bonds, with some contributions of C-N stretching
224 vibrations, respectively. The amide III at 1200 cm^{-1} was a complex band assigned to an in-phase
225 combination of N-H in plane bending, C-N stretching vibrations, C-C stretching and C=O bending
226 vibrations (Cardamone, 2008), but it also depended on the nature of the side-chain groups and
227 hydrogen bonding (Jackson & Mantsch, 1995). Finally, the intense peak at 1025 cm^{-1} was
228 attributed to the stretching vibration of the Bunte's salt residues (Erra et al., 1997).

229 Citric acid has IR band at 3291 cm^{-1} associated with the OH stretching mode. The two strong
230 bands at 1745 and 1698 cm^{-1} are assigned to C=O stretching modes. The bands at 1389 , 1242 ,
231 1174 , 1140 cm^{-1} corresponding to C-O stretching modes (Bichara, Lanús, Ferrer, Gramajo &
232 Brandán, 2011).

233 The spectrum of the film of keratin with citric acid shows an overlapping of the two previously
234 described spectra. It is possible to notice one additional peak at 1716 cm^{-1} compared to the
235 spectrum of pure keratin due to the presence of citric acid with variation in the wavenumber in the
236 neighboring peaks. In order to study the effect of citric acid in the keratin protein, the peak of
237 amide I was analyzed, because this band is known to be sensitive especially to the secondary
238 structure of proteins (Surewicz, Mantsch & Chapman, 1993). Citric acid is known for its high
239 capacity to generate hydrogen bonds (Ortega-Toro, Collazo-Bigliardi, Talens & Chiralt, 2016;
240 Ghanbarzadeh, Almasi & Entezami, 2011; Reddy & Yang, 2010; Shi et al., 2008; Jiugao, Ning &
241 Xiafoei, 2005) and its presence could change the content of macromolecular structure of keratin.

242 The peak of amide I was resolved into Gaussian bands, which number was defined by the second
243 order derivative spectrum (Figure 6 (a)). Consequently, at these bands were assigned their
244 correspondent area percentage (calculated respected to the total peak area). Furthermore, the peak
245 of amide II was analyzed (Figure 6 (b)) in order to verify the results of content of macromolecular
246 structure by using the amide I, because amide II peak is well known due to this band also can be
247 sensitive especially to the secondary structures in proteins (Miyazawa & Blout, 1961; Vedantham,
248 Gerald Sparks, Sane, Tzannis & Przybycien, 2000; Adochitei & Drochioiu, 2011).

249 In Figure 6, it is possible to observe the fitting peaks with Gaussians. Their area percentages
250 were used to determine the amount of molecular structure of alpha helix, beta sheet, side chains,
251 disordered and any additional contribution. In order to make this analysis, it was necessary to
252 obtain the contribution of citric acid and amide I separated. The contribution corresponding only
253 at amide I was compared with results reported in previous works (Aluigi et al., 2007; Aluigi,
254 Corbellini, Rombaldoni, Zoccola & Canetti, 2013), as listed in Table 3. Furthermore, the results
255 for amide II are reported in the Table 4.

256
257 Analyzing the information of the Table 3 it is possible to note that reductions in the content of
258 side chain, beta sheet and disordered/turn values are probable. Nevertheless, a growth in the alpha
259 helix structure is present. These results were confirmed when amide II peak was also fitted with
260 Gaussians (Table 4).

261 On the other hand, it is well known that alpha and beta structures are stabilized by hydrogen
262 bonds between NH and CO groups of the polypeptide chains. In addition, two or more alpha helices
263 can entwine to form a very stable structure. Such as, alpha-helical coiled coils are found in myosin
264 and tropomyosin in muscles, in fibrin in blood clots, and in keratin in hair. The helical cables in
265 these proteins have a mechanical role in forming stiff bundles of fibers (Berg, Tymoczko & Stryer,

266 2002). From this point of view, changes in the molecular conformation of alpha helix and beta
267 sheet are likely due to the high content of hydrogen bonds originating in citric acid that can replace
268 the hydrogen bonds present between different keratin chains and between keratin chain and water
269 molecules. In this way, the growth of alpha helix and the decrease in all other structure are possible.

270 In addition, the mechanical response of alpha-keratin has been extensively studied and shows,
271 in some cases, a high elastic deformation (Wang, Yang, McKittrick & Meyers, 2016). As a result,
272 mechanical properties of the keratin/citric acid film improve in comparison to films of pure keratin
273 (Aluigi et al., 2007), which is probably consequence of high content of alpha structure originating
274 in citric acid. In addition, the tensile strength could be increased by thermal treatment because of
275 changes in the moisture content and the amount of reticulation in the protein chains of keratin.

276 3.5. Antibacterial test

277 Antimicrobial action of citric acid has been reported in literature (In, Kim, Kim & Oh, 2013;
278 Pundir, & Jain, 2011). In this work, the biocidal effect of citric acid was evaluated on the film
279 following the AATCC 100 Test Method against *S. aureus* (Gram positive). The test confirmed an
280 excellent antibacterial property of the film, before and after immersion in water at 5 and 60
281 minutes, with a bacterial reduction of 100%.

282 3.6. Qualitative assessment carrot shelf-life

283 In the Figure 7 the results of carrot preservation with a film for preserving food and keratin/citric
284 acid film are reported. Firstly, in the control sample, the carrot suffered mainly a drying process
285 that can be observed from the first day and it is kept up eleven subsequent days. Using the film for
286 preserving food, carrot has been conserved for one day, but after eleven days it suffered a drying
287 and oxidation process that is evidenced by the dark color of the surface. Finally, in the case of
288 carrot packed with the keratin/citric acid film, after the first day carrot has been conserved but it

289 released a little amount of water that was evidenced in the support paper underneath it. After eleven
290 days, carrot seemed to be conserved with a change in the physic form that could correspond a
291 drying process. At the end of the test, after 51 days, the observations are confirmed. As a result,
292 the effect of citric acid contented in the film on the carrot surface and on the qualitative assessment
293 carrot shelf-life is noticeable. This film can qualitatively improve the preservation of food and
294 reduce oxidation processes. It demonstrates the possible application of the keratin/citric acid film
295 for food packaging as a substitute of synthetic polymers, replacing them with a renewable source.

296

297 **4. Conclusion**

298 In conclusion, it is possible to produce by casting a plasticized wool keratin/citric acid film with
299 good characteristics of transparency and antibacterial properties. Citric acid promotes the
300 formation of macromolecular arrangements of keratin rich in alpha helix that leads to a molecular
301 structure with improved elongation and flexibility in the film. The resulting material presents high
302 value of elongation at break (higher than 600%) under mechanical tests. Moreover, the film shows
303 an inherently and complete biocidal action. Additionally, the immersion of this film in water
304 showed a small keratin loss (10% wt.) and almost complete citric acid loss. Finally, it was
305 demonstrated that this film can qualitatively improve the shelf-life of carrot. As a result,
306 keratin/citric acid films can be used as substitute of synthetic polymers for packaging, replacing
307 fossil fuels with renewable sources and bio-based products in plastic goods. Therefore, this
308 material could have practical applications in food industry as active packaging.

309 *Acknowledgements*

310 This research did not receive any specific grant from funding agencies in the public, commercial,
311 or not-for-profit sectors.

313 **REFERENCES**

314 Adochitei, A. & Drochioiu, G. (2011). Rapid Characterization of Peptide Secondary Structure
315 by FT-IR Spectroscopy. *Rev. Roum. Chim.*, 56(8), 783-791.

316 Aluigi, A., Zoccola, M., Vineis, C., Tonin, C., Ferrero, F. & Canetti, M. (2007). Study on the
317 structure and properties of wool keratin regenerated from formic acid. *Int. J. Biol. Macromol.*, 41,
318 266-73.

319 Aluigi, A., Vineis, C., Tonin, C., Tonetti, C., Varesano, A. & Mazzuchetti, G. (2009). Wool
320 keratin-based nanofibres for active filtration of air and water. *J. Biobased Mater. Bioenergy*, 3,
321 1-9.

322 Aluigi, A., Tonetti, C., Vineis, C., Tonin, C. & Mazzuchetti, G. (2011). Adsorption of copper
323 (II) ions by keratin/PA6 blend nanofibres. *Eur. Polym. J.* 47, 1756-1764.

324 Aluigi, A., Tonetti, C., Vineis, C., Varesano, A., Tonin, C. & Casasola, R. (2012). Study on the
325 adsorption of chromium (VI) by hydrolyzed keratin/polyamide 6 blend nanofibres. *J. Nanosci.*
326 *Nanotechnol.* 12, 7250-9.

327 Aluigi, A., Corbellini, A., Rombaldoni, F., Zoccola, M. & Canetti, M. (2013). Morphological and
328 structural investigation of wool-derived keratin nanofibres crosslinked by thermal treatment. *Int.*
329 *J. Biol. Macromol.* 57, 30-37.

330 Aluigi, A., Rombaldoni, F., Tonetti, C. & Jannoke, L. (2014). Study of methylene blue
331 adsorption on keratin nanofibrous membranes. *J. Hazard. Mater.*, 268, 156-165.

332

333 Appendini, P. & Hotchkiss, J.H. (2002). Review of antimicrobial food packaging. *Innovative*
334 *Food Sci. Emerging Technol.* 3 113–126.

335 Barbooti, M.M. & Al-Sammerrai, D.A. (1986). Thermal decomposition of citric acid.
336 *Termochimica Acta.*, 98, 119-126.

337 Berg, J.M., Tymoczko, J.L. & Stryer, L. (2002). Secondary Structure: Polypeptide Chains Can
338 Fold Into Regular Structures Such as the Alpha Helix, the Beta Sheet, and Turns and Loops. *In*
339 *Biochemistry Section 3.3* ; 5th edition; W H Freeman: New York, .
340 <http://www.ncbi.nlm.nih.gov/books/NBK22580/> Accessed 03.04.16.

341 Bichara, L.C., Lanús, H.E., Ferrer, E.G., Gramajo, M.B. & Brandán, S.A. (2011). Vibrational
342 study and force field of the citric acid dimer based on the SQM methodology. *Adv. Phys. Chem.*,
343 *2011*, 1-10.

344 Cardamone, J. M. (2008). Keratin transamidation. *Int. J. Biol. Macromol.*, 42, 413-9.

345 Caro, N., Medina, E., Díaz-Dosque, M., López, L. & Abugoch, L. (2016). Novel active
346 packaging based on films of chitosan and chitosan/quinoa protein printed with chitosan-
347 tripolyphosphate-thymol nanoparticles via thermal ink-jet printing. *Food hydrocolloids*, 52, 520-
348 532.

349 Erra, P., Gomez, N., Dolcet, L. M., Julia, M. R., Lewis, D.M. & Willoughby, J. H. (1997). FTIR
350 analysis to study chemical-changes in wool following a sulfitolysis treatment. *Text. Res. J.*, 67,
351 397-401.

352 Fabra, M.J., López-Rubio, A. & Lagaron, J.M. (2016). Use of the electrohydrodynamic process
353 to develop active/bioactive bilayer films for food packaging applications. *Food hydrocolloids*, 55,
354 11-18.

355 Fraser, R. D. B., MacRae, T. P. & Rogers, G. E. (1972). *Keratins: Their Composition, Structure*
356 *and Biosynthesis*. (pp. 23). Thomas: Springfield, IL.

357 Ghanbarzadeh, B., Almasi, H. & Entezami, A.A. (2011). Improving the barrier and mechanical
358 properties of corn starch-based edible films: Effect of citric acid and carboxymethyl cellulose. *Ind.*
359 *Crops Prod.*, 33, 229-235.

360 Hegyi, G., Kardos, J., Kovacs, M., Malnasi-Csizmadia, A., Nyitray, L., Pal, G., Radnai, L.,
361 Reményi, A. & Venekei, I. (2013). Absorption spectrum of protein. In *Introduction to Practical*
362 *Biochemistry- Section 4.6.4* [Online]; Eotvos Lorand University.
363 [http://elte.prompt.hu/sites/default/files/tananyagok/IntroductionToPracticalBiochemistry/index.ht](http://elte.prompt.hu/sites/default/files/tananyagok/IntroductionToPracticalBiochemistry/index.html)
364 [ml](http://elte.prompt.hu/sites/default/files/tananyagok/IntroductionToPracticalBiochemistry/index.html) Accessed 03.04.16.

365 Held, P. (2016). BioTek. Applications – Application notes: Peptide and amino acid
366 quantification using UV fluorescence in synergy HT multi-mode microplate reader.
367 <http://www.biotek.com/resources/articles/peptides-amino-acids-fluorescence.html> Accessed
368 03.04.16.

369 In, Y.W., Kim, J.J., Kim, H.J. & Oh, S.W. (2013). Antimicrobial activities of acetic acid, citric
370 acid and lactic acid against shigella species. *J. Food Saf.*, 33, 79-85.

371 Jackson, M. & Mantsch, H. H. (1995). The use and misuse of FTIR spectroscopy in the
372 determination of protein structure. *Crit. Rev. Biochem. Mol. Biol.*, 30, 95-120.

373 Jiugao, Y., Ning, W. & Xiafoei, M. (2005). The effects of citric acid on the properties of
374 thermoplastic starch plasticized by glycerol. *Starch.*, 57, 494-504.

375 Long, N.N.V. Joly, C. & Dantigny, P. (2016). Active packaging with antifungal activities. *Int.*
376 *J. Food Microbiol.*, 220, 73-90.

377 Miyazawa, T. & Blout, E.R., (1961). The Infrared Spectra of Polypeptides in Various
378 Conformations: Amide I and II bands. *J. Am. Chem. Soc.*, 83, 712-719.

379 Ortega-Toro, R., Collazo-Bigliardi, S., Talens, P. & Chiralt, A. (2016). Influence of citric acid
380 on the properties and stability of starch-polycaprolactone based films. *J. appl. Polym. Sci.*, 42220.

381 Petersen, K., Nielsen, P.V. & Olsen, M.B. (2001). Physical and mechanical properties of
382 biobased materials-starch, polylactate and polyhydroxybutyrate. *Starch.*, 53, 356-361.

383 Pundir, R.K. & Jain, P. (2011). Evaluation of five chemical food preservatives for their
384 antibacterial activity against bacterial isolates from bakery products and mango pickles. *J. Chem.*
385 *Pharm. Res.*, 3, 24-31.

386 Reddy, N. & Yang, Y. (2010). Citric acid cross-linking of starch films. *Food Chem.*, 118, 702-
387 711.

388 Schmid, F.X. (2001). Biological Macromolecules: UV-visible spectrophotometry, *eLs.*

389 Shi, R., Bi, J., Zhang, Z., Zhu, A., Chen, D., Zhou, X., Zhang, L. & Tian, W. (2008). The effect
390 of citric acid on the structural properties and cytotoxicity of polyvinyl alcohol/starch films when
391 molding at high temperature. *Carbohydr. Polym.*, 74, 763-770.

392 Soccol, C.R., Vandenberghe, L.P.S., Rodrigues, C. & Pandey, A. (2006). New perspectives for
393 citric acid production and applications. *Food Technol. Biotechnol.*, 44, 141-149.

394 Surewicz, W.K., Mantsch, H.H. & Chapman, D. (1993). Determination of protein secondary
395 structure by fourier transform infrared spectroscopy: a critical assessment. *Biochemistry.*, 32, 389-
396 94.

397 Tachibana, A., Furuta, Y., Takeshima, H., Tanabe, T. & Yamauchi, K. (2002). Fabrication of
398 wool keratin sponge scaffolds for long-term cell cultivation. *J. Biotechnol.*, 93, 165-170.

399 Tachibana, A., Kaneko, S., Tanabe, T. & Yamauchi, K. (2005). Rapid fabrication of keratin-
400 hydroxyapatite hybrid sponges toward osteoblast cultivation and differentiation. *Biomaterials*, 26,
401 297-302.

402 Varesano, A., Vineis, C., Tonetti, C., Sanchez Ramirez, D.O., Mazzuchetti, G. (2014). Chemical
403 and physical modifications of electrospun keratin nanofibers induced by heating treatments. *J.*
404 *Appl. Polym. Sci.* 40532.

405 Varesano, A., Vineis, C., Tonetti, C., Sanchez Ramirez, D.O., Mazzuchetti, G., Ortelli, S., Blosi,
406 M. & Costa, A.L. (2015). Multifunctional hybrid nanocomposite nanofibers produced by colloid
407 electrospinning from water solutions. *Curr. Nanosci.*, 11, 41-48.

408 Vedantham, G., Gerald Sparks, H., Sane, S.U., Tzannis, S. & Przybycien, T.M. (2000). A
409 Holistic Approach for Protein Secondary Structure Estimation from Infrared Spectra in H₂O
410 Solutions. *Analytical Biochemistry.*, 285, 33-49.

411 Wang, B., Yang, W., McKittrick, J. & Meyers, M.A. (2016). Keratin: structure, mechanical
412 properties, occurrence in biological organisms, and efforts at bioinspiration. *Prog. Mater. Sci.*, 76,
413 229-318.

414 Yamauchi, K., Maniwa, M. & Mori, T. (1998). Cultivation of fibroblast cells on keratin-coated
415 substrata. *J. Biomater. Sci. Polym.*, Ed. 9, 259.

416

417 **Figure captions**

418 **Figure 1.** (a) Spectrum UV-VIS of keratin/citric acid film; (b) Picture of the keratin/citric acid
419 film.

420 **Figure 2.** Absorbance values in UV-VIS of water after film immersion with dilution 1:10 at
421 different times (a) 275 nm, related to aromatic rings of proteins in water; (b) 214 nm, related to
422 carboxylic groups of both citric acid and peptide bonds.

423 **Figure 3.** Thermal graphs for pure keratin and keratin/citric acid film. (a) TGA pure keratin and
424 keratin/citric acid film; (b) and (d) DTG and DSC for pure keratin, respectively; (c) and (e) DTG
425 and DSC for keratin/citric acid film, respectively.

426 **Figure 4.** Tensile strength test of keratin/citric acid film. On the right: at the beginning of the test;
427 on the left: before the film breaking.

428 **Figure 5.** Spectrum FT-IR of keratin/citric acid film, pure keratin and pure citric acid

429 **Figure 6.** Fitting peaks with Gaussians in amide I (a) and amide II (b)

430 **Figure 7.** Carrot shelf-life: film for preserving food (Film (a)) and keratin/citric acid film (Film
431 (b)) in comparison with a piece of unpacked carrot (Control)

Tables

Table 1. Results after 2 h water immersion at different volumes.

	20 ml	5 ml
Total lost weight (%)	56 ± 5	57 ± 5
Lost citric acid (%)	92 ± 8	97 ± 3
Lost keratin (%)	12 ± 3	6 ± 1
Protein concentration (g l⁻¹)	0.28 ± 0.06	0.46 ± 0.11
pH*	2.88 ± 0.03	2.61 ± 0.12

*The initial pH of water was 5.96 (20°C).

Table 2. Values of tensile strength test

Thermal treatment conditions	Tensile strength (MPa)	Elongation at break (%)
As cast (untreated)	0.28 ± 0.19	646 ± 177
80 °C – 1 h	0.37 ± 0.19	366 ± 151
100 °C – 1 h	0.70 ± 0.36	317 ± 24
120 °C – 1 h	1.49 ± 0.80	138 ± 21

Table 3. The result of Fitting peaks with Gaussians in amide I peak

Band assignment	Keratin-Citric acid 15% wt. (water) ^(a)		Keratin 5%wt. (water) ^(b)		Keratin 5%wt. (formic acid) ^(b)		Keratin 15%wt. (formic acid) ^(c)	
	Band position (cm ⁻¹)	Content (%)	Band position (cm ⁻¹)	Content (%)	Band position (cm ⁻¹)	Content (%)	Band position (cm ⁻¹)	Content (%)
Side chains or other	1597	0.1	1596	1	1597 1586	8	1592	8
Beta sheet	1618	29.5	1620	33	1621	42	1621	36
Alpha helix	1651	58.1	1649	47	1650	26	1650	27
Disordered/turns	1674	12.4	1674	19	1675	22	1678	22
	1682		1691		1697			
	1691							
Other or COOH					1725	2	1725	7

^(a) Present work, ^(b) Aluigi et al., 2007, ^(c) Aluigi, Corbellini, Rombaldoni, Zoccola & Canetti, 2013.

Table 4. The result of fitting peaks with Gaussians in amide II peak

Keratin-Citric acid 15% wt. (water)		
Band assignment	Band position (cm⁻¹)	Content (%)
Other	1502	4.7
Random coil	1535	1.0
Beta sheet	1524	29.3
	1529	
	1556	
Alpha helix	1516	59.1
	1541	
Turns	1549	5.9
	1564	

Figure graphics

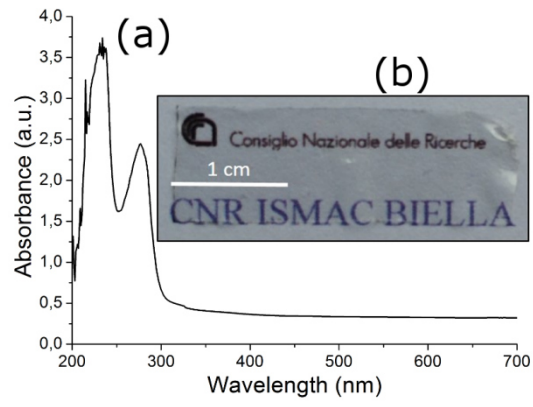


Figure 1

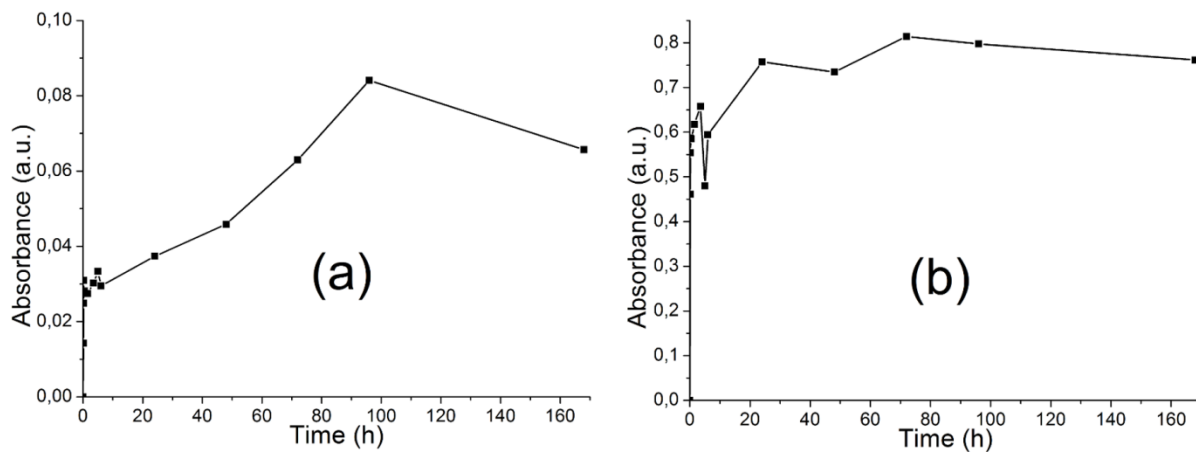


Figure 2

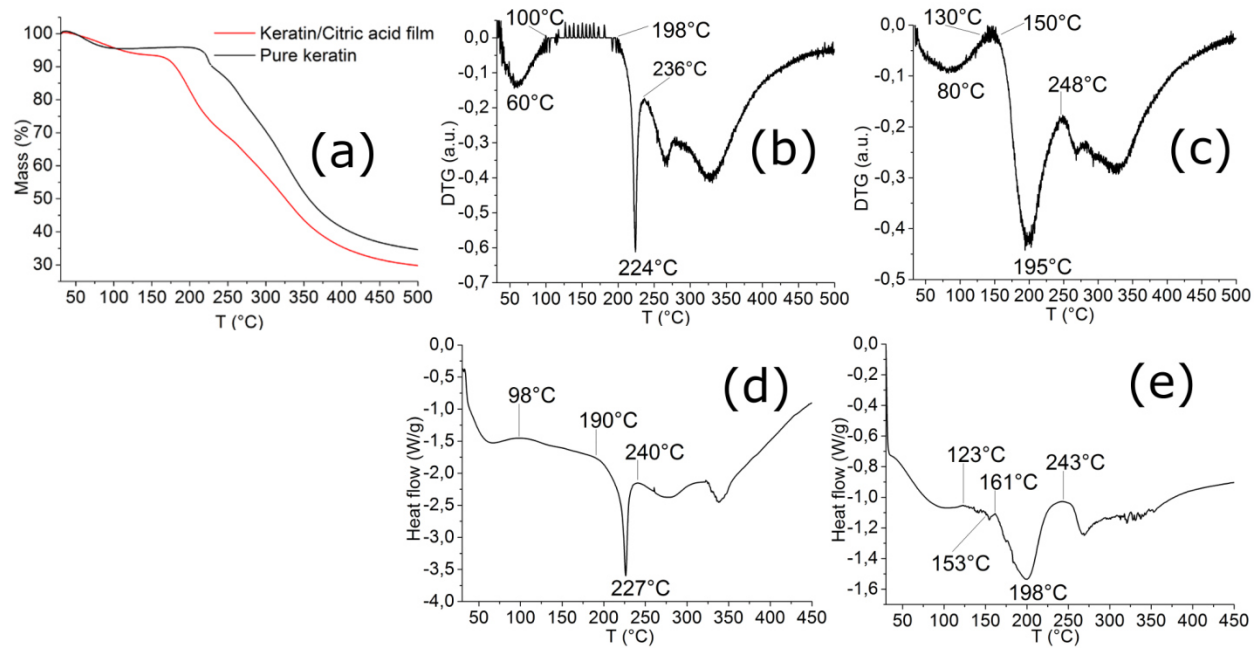


Figure 3



Figure 4

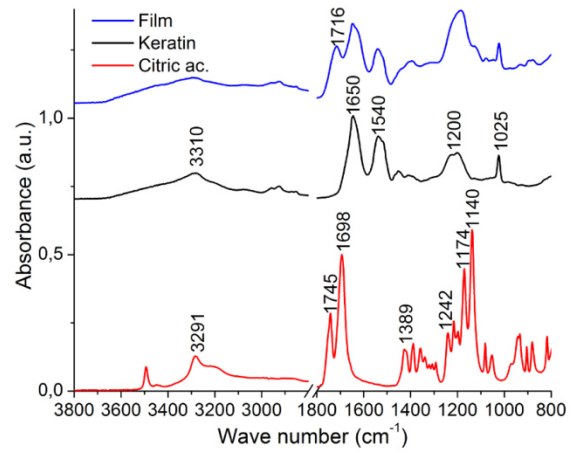


Figure 5

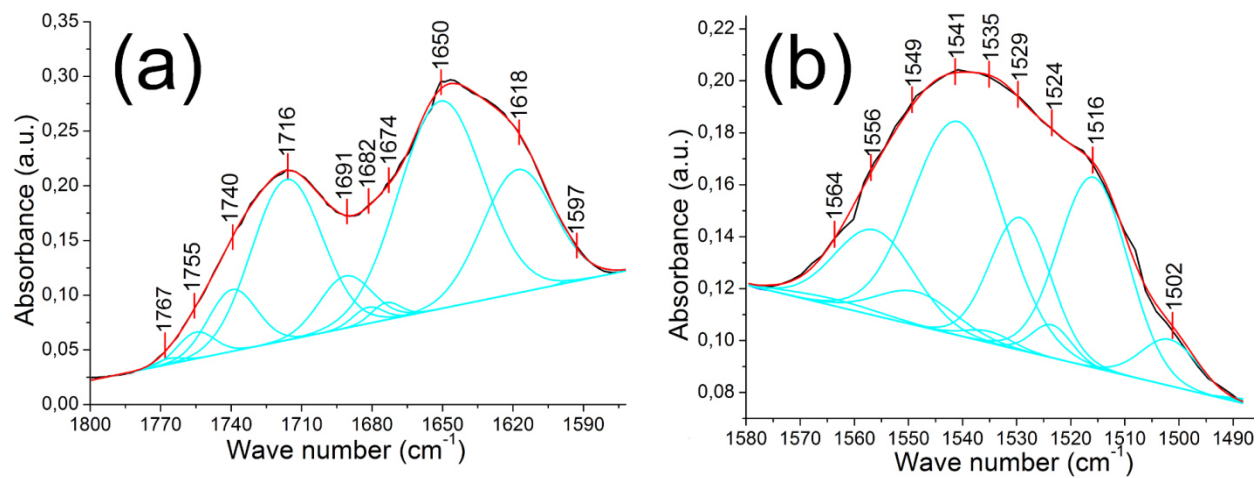


Figure 6



Figure 7

432

433